Macromolecules

Article

pubs.acs.org/Macromolecules

An Investigation of Polyamides Based on Isoidide-2,5-dimethyleneamine as a Green Rigid Building Block with Enhanced Reactivity

Jing Wu,[†,○,⊥] Lidia Jasinska-Walc,*[,†,⊥,§] Dmytro Dudenko,[∥] Artur Rozanski,[‡] Michael Ryan Hansen,*[,∥] Daan van Es,[○,⊥] and Cor E. Koning[†,⊥,#]

[†]Laboratory of Polymer Materials, Eindhoven University of Technology, Den Dolech 2, P.O. Box 513, 5600 MB Eindhoven, The Netherlands

[⊥]Dutch Polymer Institute DPI, PO Box 902, 5600 AX Eindhoven, The Netherlands

[§]Department of Polymer Technology, Chemical Faculty, Gdansk University of Technology, G. Narutowicza Str. 11/12, 80-952 Gdansk, Poland

[∥]Max Planck Institute for Polymer Research, Ackermannweg 10, 55128 Mainz, Germany

[‡]Centre of Molecular and Macromolecular Studies, Polish Academy of Sciences, Sienkiewicza 112, 90-363 Lodz, Poland

[○]Food & Biobased Research, Wageningen University and Research Center, Bornse Weilanden 9, 6708 WG Wageningen, The Netherlands

[#]DSM Coating Resins, Ceintuurbaan 5, Zwolle, The Netherlands

Supporting Information

ABSTRACT: Novel, semicrystalline polyamides and copolyamides were synthesized from a new carbohydrate-based diamine, namely isoidide-2,5-dimethyleneamine (IIDMA). In combination with 1,6-hexamethylene diamine (1,6-HDA) as well as the biobased sebacic acid (SA) or brassylic acid (BrA), the desired copolyamides were obtained via melt polymerization of the nylon salts followed by a solid-state polycondensation (SSPC) process. Depending on the chemical compositions, the number average molecular weights (M_n) of the polyamides were in the range of 4000−49000 g/mol. With increasing IIDMA content in the synthesized copolyamides, their corresponding glass transition temperatures (T_g) increased from 50 °C to approximately 60−67 °C while the melting temperatures (T_m) decreased from 220 to 160 °C. The chemical structures of the polyamides were analyzed by NMR and FT-IR spectroscopy. Both differential scanning calorimetry (DSC) and wide-angle X-ray diffraction (WAXD) analyses revealed the semicrystalline character of these novel copolyamides. Variable-temperature (VT) $^{13}C\{^1H\}$ cross-polarization/magic-angle spinning (CP/MAS) NMR and FT-IR techniques were employed to study the crystal structures as well as the distribution of IIDMA moieties over the crystalline and amorphous phases of the copolyamides. The performed *ab initio* calculations reveal that the stability of the IIDMA moieties is due to a pronounced "boat" conformation of the bicyclic rings. The incorporation of methylene segments in between the isohexide group and the amide groups enables the hydrogen bonds formation and organization of the polymer chain fragments. Given the sufficiently high T_m values (~200 °C) of the copolyamides containing less than 50% of IIDMA, these biobased semicrystalline copolyamides can be useful for engineering plastic applications.

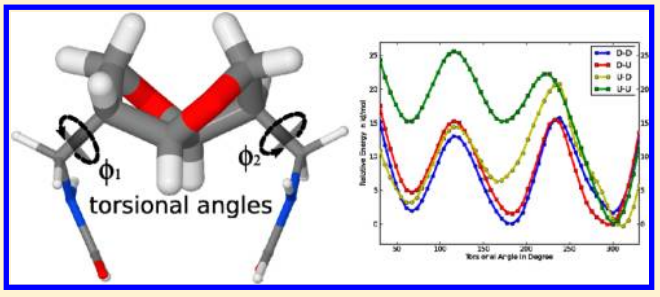

INTRODUCTION

The various commercially available polyamides (PAs) belong to one of the most important classes of semicrystalline polymers owing to their good thermal and mechanical properties. Concerning the versatile applications of PAs, often in demanding conditions, some naturally occurring polyamides formed from amino acids, e.g., wool or silk, can be used for textile production. Recently, PAs such as PA 6.6, PA 6, and PA 6.10 have gradually substituted wool and silk and have been applied in a wide range of applications. Nowadays, owing to their excellent physicochemical and mechanical properties, PAs form one of the most important groups of step-growth polymers, and are extensively used in industry for injection molding, extrusion and film or fiber applications. Nevertheless, a fundamental fact one should realize is that all developments in the polyamide industry cannot be continued and not even be maintained without the abundant availability of raw materials, which are typically fossil resource based.

Received: October 10, 2012
Revised: November 13, 2012
Published: November 19, 2012

   dx.doi.org/10.1021/ma302126b | *Macromolecules* 2012, 45, 9333−9346

Scheme 1. Strategies for Generating Novel Isohexide-Based Diamines from the Parent Isohexides

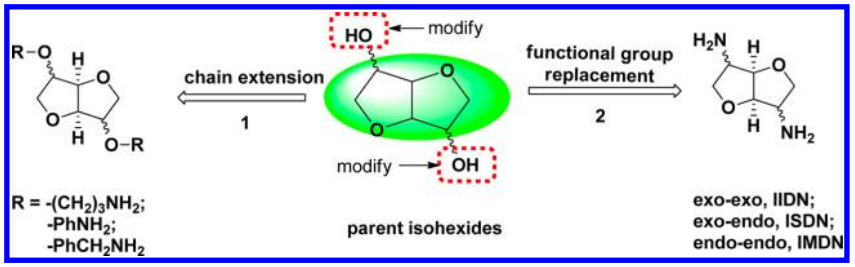

With the growing concern of the fossil feed stock shortage and the relating environmental issues of fossil feed stock consumption, biomass is regarded as a promising resource for producing sustainable chemicals, fuels and energy. Among numerous existing biomass monomers, the carbohydrate-derived 1,4:3,6-dianhydrohexitols (isohexides) are highly interesting building blocks for step-growth polymerization.[1−3] Isohexides are a group of rigid secondary diols derived from C6-sugars, which are found in three major isomeric forms, namely isosorbide (1,4:3,6-dianhydro-D-glucitol, IS, with 2-*endo*, 5-*exo* oriented hydroxyl groups), isomannide (1,4:3,6-dianhydro-D-mannitol, IM, with 2-*endo*, 5-*endo* oriented hydroxyl groups) and isoidide (1,4:3,6-dianhydro-L-iditol, II, with 2-*exo*, 5-*exo* oriented hydroxyl groups).[4−7] These molecules can be obtained from starch or cellulose via few (bio)organic transformations and therefore are considered as biogenic. In recent years, extensive interests raised from both academia and industry focusing on the utilization of isohexides for various types of step-growth polymers, such as polyesters, polyamides, polycarbonates and polyurethanes.[1−3] One of the most appealing features of the isohexides is their intrinsic rigidity originating from the bicyclic rings, which can significantly enhance the glass transition temperature (T_g) and thereby broaden the application window of polymers. Such effects have been demonstrated by several authors for the isohexide-modified poly(ethylene terephthalate) (PET)[8−11] and poly(butylene terephthalate) (PBT)[12] as well for succinic-acid based powder coatings.[13−16] The potential industrial applications of the isohexide-based polymers encompass packaging, (powder) coating resins, and performance polymers as well as optical or biomedical materials.[1−3,17−21]

Despite these promising and unique properties of isohexides, the relatively poor reactivity of their secondary hydroxyl groups at the 2- and 5-positions (see Scheme 1) has been recognized as a major drawback, which often results in low molecular weights (MW) and severely colored polymers.[11,15,22] Moreover, as bifunctional alcohols, the parent isohexide apparently is limited to be directly used as monomer for the synthesis of certain types of step-growth polymers, e.g., PAs. Hence, a number of isohexide-derivatives have been reported for better reactivity and/or diverse functionalities.[1−3,20]

In order to synthesize PAs, the parent isohexide has been transformed into amino-derivatives through chain extension on the oxygen atom of the 2/5-hydroxyl groups (−OH) by, e.g., propylamine ($-(CH_2)_3NH_2$), phenylamine ($-PhNH_2$) or benzylamine ($-PhCH_2NH_2$) (strategy 1, Scheme 1),[23−26] or through the direct replacement of the 2/5-hydroxyl groups by amine ($-NH_2$) groups (strategy 2, Scheme 1).[27−30] Since the functional groups are directly attached to the bicyclic skeleton of isohexide, the latter strategy has been proven to be able to retain the structural rigidity to a large extent.[31] Following such a strategy, thus far three isomeric isohexide-based diamines have been generated, namely diaminoisosorbide (DAIS), diaminoisomannide (DAIM), and diaminoisoidide (DAII). Thiem et al.[28] reported the first PAs derived from these isohexide-based diamines in combination with several aromatic or aliphatic diacyl chlorides via interfacial polymerization.[28] These PAs show high degrees of polymerization and T_g values in the range of 50−70 °C, which are significantly higher than those of commercially available PA 6 or PA 6.6. Recently, our studies on isohexide-derived PAs[17−19] presented the comprehensive analyses concerning the preparation of series of fully biobased copolyamides (co-PAs) by incorporating DAII or DAIS into PA 4.10 or PA 4.13. The synthetic protocol, starting with the preparation of the corresponding nylon salts, combines a conventional melt-polymerization with a solid-state postpolycondensation (SSPC), affording the desired co-PAs with number-average molecular weights (M_n) above 20 000 g/mol. In comparison to PA 4.10 or PA 4.13, these isohexide-derived co-PAs exhibit lower degrees of hydrogen bond density and thus have lower melting points.

We are interested in developing versatile isohexide-based building blocks as well as in their applications in step-growth polymerization. Recently, with the aim to develop novel isohexide derivatives with improved reactivity and preserved rigidity, we reported a new family of isohexide-based bifunctional monomers following the second strategy presented in Scheme 1.[31] The original hydroxyl groups were replaced by several 1-carbon extended functionalities including carboxylates ($-COOH$, $-COOCH_3$), methylenehydroxyl ($-CH_2OH$) and methyleneamine ($-CH_2NH_2$).[31] Subsequently, several partially or fully biobased polyesters from these building blocks, including isoidide dicarboxylic acid (IIDCA) and isoidide dimethanol (IIDML), were synthesized.[21] The sufficiently high molecular weights (M_n = 10 000−30 000 g/mol) as well as the appropriate thermal properties of the resulting polyesters revealed the improved reactivity and largely preserved structural rigidity of the novel monomers.

In this work, we present a series of copolyamides based on a novel one-carbon extended isohexide diamine, namely isoidide-2,5-dimethylene amine (IIDMA), which can be synthesized from isomannide via a dinitrile intermediate (IIDN) (Scheme 2).[31] Compared to the known secondary isohexide-based diamines, like diaminoisoidide (DAII) or diaminoisosorbide (DAIS), IIDMA is a primary diamine and therefore is expected to exhibit higher reactivity. In this work, the synthesis, chemical structure characterization, thermal properties and crystal structure analysis of the PAs based on IIDMA, 1,6-hexamethylene diamine (1,6-HDA) and the biobased dicarboxylic acids, including sebacic acid (SA) and brassylic acid (BrA) produced from castor oil and erucic acid, will be described. The chemical structure of the synthesized PAs was characterized by nuclear magnetic resonance (NMR) spectroscopy. In addition,

dx.doi.org/10.1021/ma302126b | *Macromolecules* 2012, 45, 9333−9346

Scheme 2. Chemical Structure of Isoidide Dimethylene Amine (IIDMA) Prepared from Isomannide via the Dinitrile Intermediate[a]

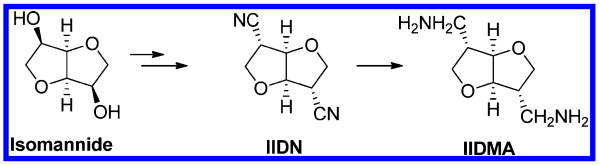

[a]For detailed reaction conditions and yields, see Experimental Section.

FT-IR spectroscopy, wide-angle X-ray scattering (WAXD) and solid-state NMR spectroscopy were employed to elucidate the hydrogen bonding nature and chain packing capabilities as well as the distribution of IIDMA over the crystalline and amorphous phases of the PAs.

EXPERIMENTAL SECTION

Materials. ((3*S*,6*S*)-Hexahydrofuro[3,2-b]furan-3,6-diyl)-dimethanamine (IIDMA) was prepared according to the published method.[31] The following chemicals and solvents were used as received unless stated otherwise: isomannide (Sigma-Aldrich), trifluoromethanesulfonic anhydride (≥99%, Aldrich), dichloromethane (Merck, p.a.), pyridine (Merck, p.a.), tetrahydrofuran (anhydrous, ≥99.9%, Sigma-Aldrich), potassium cyanide (extra pure, Merck), 18-crown-6 (≥99%, Fluka), chloroform (Merck, p.a.), borane−tetrahydrofuran complex (BH_3-THF) in THF solution (1.0 M, Sigma-Aldrich), hydrochloride in diethyl ether solution (2.0 M, Sigma-Aldrich), 1,6-hexamethylene diamine (98%, Sigma-Aldrich), sebacic acid (99%, Sigma-Aldrich), brassylic acid (1,11-undecanedicarboxylic acid, Sigma-Aldrich, 94%, purified by recrystallization from toluene), chloroform-*d* (99.8 atom % D), trifluoroacetic acid-*d*, (99.5 atom % D, Sigma-Aldrich, TFAA), DMSO-d_6 (99.8 atom % D, Sigma-Aldrich) D_2O (>99.8 atom %, Merck), methanol-d_4 (99.8 atom % D, contains 0.05% (v/v) TMS, Aldrich), 1,1,1,3,3,3-hexafluoro-2-propanol (HFIP, Biosolve), activated carbon (Norit, CN1), magnesium sulfate (Acros Organics, 99% extra pure, dried, contains 3−4 mol of water), Celite 545 coarse (Fluka), and Amberlyst A26 (Aldrich) hydroxide form (strongly basic, macroreticular resin with quaternary ammonium functionality from Rohm and Haas Co; prior to use, the resin was washed with demineralized water by sonication in an ultrasonic bath at room temperature for 10 min. The water layer was subsequently removed by decantation. This procedure was repeated 5 times, until the water layer remained colorless).

(3*R*,6*R*)-Hexahydrofuro[3,2-*b*]furan-3,6-diyl Bis-(trifluoromethanesulfonate) (Isoidide Bistriflate, IIBTf).[31] A 500 mL 3-necked round-bottom flask, equipped with a mechanical stirrer and a dropping funnel, was charged with isomannide (36.5 g, 0.25 mol), pyridine (49 mL), and dichloromethane (150 mL). The colorless solution was cooled down to −10 °C. Next, trifluoromethanesulfonic anhydride (0.6 mol, 100 mL) was added dropwise over 1 h. After stirring at room temperature for an additional 3 h, the reaction mixture was poured onto ice−water (0.5 L) and stirred. The organic layer was separated, and the water layer was extracted with chloroform (3 × 150 mL). The combined organic layers were subsequently washed with aqueous HCl (1.0 M, 3 × 150 mL), water (2 × 150 mL), dried over $MgSO_4$, and decolorized with activated carbon. After filtration over a glass filter containing Celite, the resulting clear solution was evaporated under reduced pressure using a rotary evaporator. Finally, the pure product **IIBTf** was obtained by recrystallization from ethanol as colorless needles. Yield: 95 g, 93% (purity: 100%, GLC). Mp: 62−63 °C. ^{1}H NMR ($CDCl_3$, ppm): δ = 5.22 (dd, 2H), 4.77 (m, 2H), 4.15 (m, 4H). ^{13}C NMR ($CDCl_3$, ppm): δ = 118.48 (q, $^1J_{FC}$ = 319 Hz), 83.43, 80.32, 70.86. FT-IR: 2943, 2901, 1415, 1248, 1197, 987 cm^{-1}. HR-MS (Q-Tof), *m*/*z* [M + Na]$^+$: calcd for $C_8H_8F_6O_8S_2$, 432.9457; found, 432.9463.

(3*S*,6*S*)-Hexahydrofuro[3,2-*b*]furan-3,6-dicarbonitrile (IIDN).[31] A 250 mL three-necked round-bottom flask, equipped with a magnetic stirrer, internal thermocouple, pressure-equalizing dropping funnel, and a reflux condenser, was charged with potassium cyanide (1.43 g, 22 mmol), 18-crown-6 (5.81 g, 22 mmol), and THF (50 mL). The suspension was cooled down below 0 °C, and then a solution of **IIBTf** (8.2 g, 20 mmol) in THF (20 mL) was added dropwise over 1 h under stirring and continuous flow of nitrogen. During the course of the reaction, the internal temperature increased rapidly. After addition was complete, the reaction was stirred below 0 °C for 3 h under nitrogen. When the reaction reached completion as indicated by TLC, the reaction mixture was poured onto cold water (200 mL) and extracted with chloroform (5 × 30 mL). The combined organic layers were dried over $MgSO_4$ and decolorized with activated carbon. After filtration over a glass filter containing Celite, the resulting solution was evaporated under reduced pressure using a rotary evaporator to give the crude product as a light brown solid. Finally, pure dinitrile (**IIDN**) was obtained as a white solid by flash column chromatography (ethyl acetate: petroleum ether, 1: 2). Yield: 2.63 g, 80% (purity: 100%, GLC). Mp: 123−125 °C. ^{1}H NMR ($CDCl_3$, ppm): δ = 5.02 (s, 2H), 4.14 (s, 4H), 3.19 (m, 2H). ^{13}C NMR ($CDCl_3$, ppm): 117.22, 86.20, 70.34, 36.70. FT-IR: 2492, 2901, 2248 (C≡N), 1487, 1117, 1080, 1025, 947, 755 cm^{-1}. HR-MS (Q-Tof), *m*/*z* [M + Na]$^+$: calcd for $C_8H_8N_2O_2$, 187.0478; found, 187.0474.

((3*S*,6*S*)-Hexahydrofuro[3,2-b]furan-3,6-diyl)dimethanamine Hydrochloride Salt (IIDMA Salt).[31] A 250 mL three-necked round-bottom flask, equipped with a magnetic stirrer, pressure-equalizing dropping funnel, and a reflux condenser, was charged with BH_3−THF complex in THF solution (1.0 M, 50 mL). Next, a solution of **IIDN** (0.8 g, 4.88 mmol) in THF (20 mL) was added dropwise at room temperature under a nitrogen flow in 20 min. After addition was complete, the reaction was stirred for another 16 h. Next, methanol (30 mL) was added carefully to quench the reaction, during which hydrogen gas was released vigorously. When no more gas evolved, hydrogen chloride in diethyl ether solution (2.0 M, 30 mL) was added dropwise and a white precipitate formed immediately. The suspension was then filtered over a glass filter (G-3), and the collected gum-like solid was dried in an oven (70 °C, 1 atm.) for 1 h to give the crude diamine HCl salt as white hard solid. Finally, the pure white diamine HCl salt was obtained after repeated washing with ethanol (3 × 20 mL) and drying under vacuum (35 °C, <1 mbar). Yield: 1.19 g, 66%. ^{1}H NMR (D_2O, ppm): δ = 4.45 (s, 2H), 4.01 (m, 2H), 3.67 (m, 2H), 3.54 (d, 4H), 2.42 (m, 2H). ^{13}C NMR (D_2O, ppm): δ = 85.24, 69.79, 61.70, 49.38. FT-IR: 3364, 2917, 2883, 2851, 1601, 1213, 1060 cm^{-1}. HR-MS (Q-Tof), *m*/*z* [M-2(HCl) + H]$^+$: calcd for $C_8H_{18}N_2O_2Cl_2$, 173.1285; found, 173.1282.

((3*S*,6*S*)-Hexahydrofuro[3,2-*b*]furan-3,6-diyl)dimethanamine (IIDMA).[31] Diamine HCl salt (0.19 g, 0.78 mmol) was dissolved in demineralized water (20 mL) giving a colorless solution. To this solution was added freshly washed Amberlyst A 26-OH (0.75 g, 3.2 mmol). The resulting suspension was sonicated in an ultrasonic bath for 1 h at 30 °C. After the reaction was complete, the suspension was filtered over a glass filter (G-3) containing Celite, and the IEX-resin was washed thoroughly with water (3 × 15 mL) and methanol (3 × 15 mL). The combined clear colorless solutions were evaporated to dryness using a rotary film evaporator to afford the pure diamine (**IIDMA**) as a white solid. Yield: 0.1 g, 74.6% (purity: 99.0%, ^{1}H NMR). ^{1}H NMR (CD_3OD, ppm): δ = 4.37 (s, 2H), 3.97 (m, 2H), 3.60 (m, 2H), 2.74 (m, 4H), 2.32 (m, 2H). ^{13}C NMR (CD_3OD, ppm): δ = 87.28, 71.51, 49.94, 42.63. FT-IR: 3342, 3275, 3174, 2938, 2878, 1605, 1093 cm^{-1}. HR-MS (Q-Tof), *m*/*z* [M + H]$^+$: calcd for $C_8H_{16}N_2O_2$, 173.1285; found, 173.1281.

Isoidide-2,5-dimethylamine (IIDMA) Sebacic Acid Salt. To a solution of sebacic acid (1.2 g, 0.006 mol) in ethanol (10 mL) at 50 °C was added a solution of IIDMA (1.0 g, 0.006 mol) in an ethanol/water mixture (3 mL, 2:1, v/v) dropwise. During the addition, a precipitate was formed. The mixture was stirred at 80 °C for 1 h and then at 50 °C for 1 h. The crude product was filtered and recrystallized from an ethanol/water mixture (10:1, v/v) to afford the salt as white crystals. Yield: 1.9 g, 85%. ^{1}H NMR (D_2O, ppm): δ = 4.62 (s, 2H), 4.10 (m, 2H), 3.75 (m, 2H), 3.10 (m, 4H), 2.60 (m, 2H), 2.17 (t, 4H), 1.55 (m, 4H), 1.30 (m, 8H).

dx.doi.org/10.1021/ma302126b | *Macromolecules* 2012, 45, 9333−9346

1,6-Hexamethylene Diamine Sebacic Acid Salt. To a solution of sebacic acid (4.6 g, 0.04 mol) in ethanol (200 mL) at 50 °C was added a solution of 1,6-hexamethylene diamine (8.1 g, 0.04 mol) in ethanol (10 mL) dropwise. During the addition, a precipitate was formed. The mixture was stirred at 80 °C for 1 h and then at 50 °C for 1 h. The crude product was filtered and recrystallized from ethanol/water mixture (10:1, v/v) to afford the salt as white crystals. Yield: 11.8 g, 93%. ^{1}H NMR (D_2O, ppm): δ = 2.85 (s, 4H), 2.02 (m, 4H), 1.54 (m, 4H), 1.40 (m, 4H), 1.28 (m, 4H), 1.15 (m, 8H).

Isoidide-2,5-dimethylamine (IIDMA) Brassylic Acid Salt. To a solution of brassylic acid (1.5 g, 0.006 mol) in ethanol (20 mL) at 50 °C, a solution of IIDMA (1.0 g, 0.006 mol) in an ethanol/water mixture (3 mL, 2:1, v/v) was added dropwise. During the addition, a precipitate was formed. The mixture was stirred at 80 °C for 1 h and then at 50 °C for 1 h. The crude product was filtered and recrystallized from ethanol/water mixture (10:1, v/v) to afford the salt as white crystals. Yield: 2.0 g, 81%. ^{1}H NMR (D_2O, ppm): δ = 4.47 (s, 2H), 3.96 (m, 2H), 3.59 (m, 2H), 2.93 (m, 4H), 2.46 (m, 2H), 2.03 (t, 4H), 1.40 (m, 4H), 1.13 (m, 16H).

1,6-Hexamethylene Diamine Brassylic Acid Salt. To a solution of brassylic acid (1.5 g, 0.006 mol) in ethanol (20 mL) at 50 °C, a solution of 1,6-hexamethylene diamine (0.69 g, 0.006 mol) in ethanol (3 mL) was added dropwise. During the addition, a precipitate was formed. The mixture was stirred at 80 °C for 1 h and then at 50 °C for 1 h. The crude product was filtered and recrystallized from ethanol/water mixture (10:1, v/v) to afford the salt as white crystals. Yield: 2.1 g, 96%. ^{1}H NMR (D_2O, ppm): δ = 2.84 (t, 4H), 2.01 (t, 4H), 1.53 (m, 4H), 1.39 (m, 4H), 1.27 (m, 4H), 1.13 (m, 16H).

Synthesis of the Polyamides. A three-necked round-bottom flask, equipped with an overhead mechanical stirrer, a Dean−Stark type condenser and vigreux column, was charged with 1,6-hexamethylene diamine-sebacic acid salt (0.5 g), isoidide-2,5-dimethylamine-sebacic acid salt (0.5 g), 1,6- hexamethylene diamine (0.05 g, 0.43 mmol), isoidide-2,5-dimethylamine (0.05 g, 0.29 mmol), and Irganox 1330 (0.01 g) and the mixture was stirred at 170−175 °C for 30 min under argon atmosphere. Then the temperature was raised to 190 °C and the polycondensation process was continued for 2 h. After cooling down to room temperature, the synthesized prepolymer was isolated from the flask and ground into powder, washed with demineralized water at 80 °C, filtered and dried under reduced pressure at 80 °C. The resulting product was subsequently submitted to solid-state polymerization carried out about 20−30 °C below the melting point of the prepolymer for 5 h under Ar_2 atmosphere. Analogous conditions of the polymerization process were applied for all the investigated polyamides.

Characterization. ^{1}H NMR and ^{13}C NMR spectra were recorded at room temperature using a Varian Mercury Vx spectrometer operating at frequencies of 400 and 100.62 MHz for ^{1}H and ^{13}C, respectively. The NMR analysis of the polyamides was carried out in TFAA-*d* or DMSO-d_6. For ^{1}H NMR experiments, the spectral width was 6402.0 Hz, acquisition time 1.998 s and the number of recorded scans equal to 64. ^{13}C NMR spectra were recorded with a spectral width of 24154.6 Hz, an acquisition time of 1.300 s, and 256 scans.

Size exclusion chromatography (SEC) in hexafluoroisopropanol (HFIP) was performed on a system equipped with a Waters 1515 Isocratic HPLC pump, a Waters 2414 refractive index detector (35 °C), a Waters 2707 auto sampler, and a PSS PFG guard column followed by 2 PFG-linear-XL (7 μm, 8 × 300 mm) columns in series at 40 °C. HFIP with potassium trifluoroacetate (3 g/L) was used as eluent at a flow rate of 0.8 mL/min. The molecular weights were calculated against poly(methyl methacrylate) standards (Polymer Laboratories, M_p = 580 Da up to M_p = 7.1 × 106 Da).

The thermal stability of the polymers was determined by thermogravimetric analysis (TGA) with a TGA Q500 apparatus from TA Instruments. The samples were heated from 30 to 600 °C at a heating rate of 10 °C/min under a nitrogen flow of 60 mL/min.

Glass transition temperatures (T_g) and melting temperatures (T_m) were measured by differential scanning calorimetry (DSC) using a DSC Q100 from TA Instruments. The measurements were carried out at a heating and cooling rate of 10 °C/min from −60 °C to 180−250 °C. The transitions were deduced from the second heating and cooling curves.

Variable-temperature (VT) ^{13}C{^{1}H} cross-polarization/magic-angle spinning (CP/MAS) NMR experiments were carried out on a Bruker ASX-500 spectrometer employing a double-resonance probe for rotors with 4.0 mm outside diameter. These experiments utilized 10.0 kHz MAS and a 4 μs π/2 pulse for ^{1}H. All VT ^{13}C{^{1}H} CP/MAS NMR spectra were recorded using a CP contact time of 3.0 ms and TPPM decoupling during acquisition.[32] The temperature was controlled using a Bruker temperature control unit in the range from 30 to 180 °C. The VT ^{13}C{^{1}H} CP/MAS NMR spectra were recorded under isothermal conditions at intervals of 10 °C. A heating rate of 2 °C/min was employed between temperatures. Reported temperatures are corrected for friction- induced heating due to spinning using ^{207}Pb MAS NMR of $Pb(NO_3)_2$ as a NMR thermometer.[33] The 2D ^{1}H−^{1}H double-quantum single-quantum (DQ-SQ) correlation and ^{13}C{^{1}H} frequency-switched Lee−Goldburg hetero-nuclear correlation (FSLG-HETCOR) experiments[34,35] were recorded on a Bruker AVANCE-III 850 spectrometer using a double-resonance probe for rotors with 2.5 mm outside diameter. These experiments employed spinning frequencies of 29762 and 15000 Hz, respectively. DQ excitation was performed using the BaBa sequence and the FSLG-HETCOR experiment used a CP time of 2.0 ms.[34,35] Chemical shifts for ^{1}H and ^{13}C MAS NMR are reported relative to TMS using solid adamantane as an external reference.[36,37] CP conditions were optimized using L-alanine. All samples were annealed just below their melting temperature for 5 min under a flow of nitrogen gas before NMR analysis to remove precipitation-induced structural conformations.

Geometry optimization and ^{13}C NMR chemical shift calculations were performed within the Gaussian03 program package. The geometries of the conformations obtained by merging results from a set of 1D potential energy surface (1D-PES) scanning procedure via B97-D/6-311G**[38] were further fully optimized at the same level. The most abundant conformer with respect to energy has been proceeded for further NMR chemical shifts calculations at the B97-D/6-311G** level of theory. Further details about information on the 1D-PES procedure, comparison of B97-D and MP2 results, and the NMR chemical shift calculations are given in the Supporting Information.

Fourier transform infrared spectra (FT-IR) were obtained using a Varian 610-IR spectrometer equipped with a FT-IR microscope. The spectra were recorded in a transmission mode with a resolution of 2 cm^{-1}. PA films obtained from 1,1,1,3,3,3-hexafluoroisopropanol were analyzed on a zinc selenium disk and heated from 30 °C to temperatures slightly above the melting points of the polyamides. For this purpose a Linkam TMS94 hotstage and controller were used. The samples were cooled in 10 °C steps and reheated with the same heating steps. The spectra from the second heating run were collected. Varian Resolution Pro software version 4.0.5.009 was used for the analysis of the spectra.

Analysis of the crystalline structure of the materials was performed using wide-angle X-ray scattering measurements by means of a computer-controlled goniometer coupled to a sealed-tube source of CuKα radiation (Philips), operating at 50 kV and 30 mA. The Cu Kα line was filtered using electronic filtering and the usual thin Ni filter. The data were collected at room temperature. The 1D profiles were subsequently background-corrected and normalized. Since reflections from the different crystallographic phases frequently overlap each other, it was necessary to separate them by deconvolution. Analysis of diffraction profiles of the examined samples and peak deconvolution were performed using WAXSFit software designed by M. Rabiej at the University of Bielsko-Biała (AHT).[39] The software allows to approximate the shape of the peaks with a linear combination of Gauss and Lorentz or Gauss and Cauchy functions and adjusts their settings and magnitudes to the experimental curve with a "genetic" minimizing algorithm.

RESULTS AND DISCUSSION

Synthesis and Molecular Characterization of the IIDMA-Derived (Co)polyamides. Two series of novel (co)polyamides were synthesized from isoidide-2,5-dimethyleneamine (IIDMA) and/or 1,6-hexamethlyene diamine (1,6-HDA), in combination with either sebacic acid (SA) or brassylic acid (BrA). The synthetic protocol comprises, after making the nylon salts of both diamines with both dicarboxylic acids, a solvent-free melt polycondensation process followed by an optional solid-state postcondensation (SSPC), as described previously for the diaminioisoidide (DAII)- or diaminoisosorbide (DAIS)-derived PAs.[17,18] When the IIDMA content was below 75 mol %, the two series of PA prepolymers were obtained with M_n values ranging from 6,700−21,500 g/mol, which were further enhanced to 12 400−49 000 g/mol by SSPC (Table 1, entries 2, 3, 4, 7, 8). The SSPC temperatures are approximately 20−30 °C lower than the corresponding melting points of the prepolymers.[40] In comparison with the PAs based on the secondary diamines, viz. diaminoisoidide (DAII, *exoexo* oriented diamine) or diaminoisosorbide (DAIS, *exo/endo* oriented diamine),[17−19] the impact of the chemical structure of the primary diamine (IIDMA) on its reactivity was significant, since higher molecular weight prepolymers based on IIDMA were obtained and additionally the time of SSPC reaction was shorter than for secondary diamines-based copolymers. However, it should be taken into account that in the synthesis of DAII- and DAIS-derived copolymers 1,4-diaminobutane, instead of 1,6-hexamethylene diamine, was used. Nevertheless, the differences in the molecular weight of the prepolymers obtained using similar reaction conditions and comparable contents of the bicyclic compounds were significant. As also presented for DAII- and DAIS-based polyamides,[17,18] interfacial polymerization of the diamines and sebacoyl chloride afforded lower molecular weight materials and due to the relatively low melting point of the homopolymers, which were too low for proper polycondensation process in the solid state, SSPC did not result in further enhancement of their M_n values. Therefore, regardless of the diamine configuration, the procedure consisting of melt polymerization followed by SSPC can be considered as the most suitable route toward the family of isohexide-derived products. However, as presented in Table 1, the attempt to enhance the molecular weight of the homopolymer derived from 100% IIDMA and sebacic acid (PA 5) was not successful. Due to the relatively low melting temperature of this product (157.7 °C), the SSPC process carried out at around 140 °C proved to be ineffective. Despite the limited thermal stability of the sugar-derived monomers for high temperature polymerization processes, the applied short melt polymerization in combination with SSPC allowed the successful preparation of the PAs with minor degrees of discoloration and high molecular weights.[17−19] When comparing the weighted-in and the incorporated molar ratio of the diamines, a slight preferential incorporation of 1,6-HDA residues over IIDMA was observed. The reasons can be a lower reactivity of IIDMA and/or a lower thermal stability of IIDMA than 1,6-HDA. Nevertheless, as shown in Table 1, the applied two-step polymerization conditions lead to the successful preparation of the desired products with close to expected chemical compositions.

Table 1. Chemical Compositions, Molecular Weights, and Polydispersity Indices of the Homo- and Copolyamides Synthesized from Isoidide-2,5-dimethyleneamine (IIDMA), 1,6-Hexamethylenediamine (1,6-HDA), Sebacic Acid (SA), and Brassylic Acid (BrA)

			prepolymer		polymer after SSPC	
symbol	feed molar ratio (IIDMA/1,6-HDA)[a]	built-in molar ratio (IIDMA/1,6-HDA)[b]	M_n (g/mol)[c]	PDI[c]	M_n (g/mol)[c]	PDI[c]
SA/IIDMA/1,6-HDA-Based Polyamides						
PA1	0/100	0/100	13400	2.0	–	–
PA2	25/75	26/74	21500	2.8	48900	4.2
PA3	50/50	49/51	13300	2.1	38500	3.8
PA4	75/25	68/32	9200	2.0	12400	2.3
PA5	100/0	100/0	3900	1.2	–	–
BrA/IIDMA/1,6-HDA-Based Polyamides						
PA6	0/100	0/100	4900	1.6	17400	2.3
PA7	25/75	16/84	13060	2.3	47300	4.1
PA8	50/50	42/58	6700	1.7	13900	2.3

[a]Ratio determined by weighed-in monomers. [b]Ratio determined by ^{1}H NMR; [c]Values determined using SEC against PMMA standards in HFIP.

The molecular structure of the synthesized IIDMA-based polyamides was analyzed by ^{1}H and 2D ^{1}H−^{1}H COSY nuclear magnetic resonance (NMR) spectroscopy. As exemplified by the ^{1}H NMR spectrum of the polyamide based on IIDMA and SA (PA5) in Figure 1, all proton signals from the repeating unit of the polymer are found at the expected chemical shift values with matching multiplicities. The stereochemistry of the IIDMA moieties in PA5 can be clearly identified by the resonances of the isohexide unit: based on the 2D ^{1}H−^{1}H COSY NMR spectrum there is no ^{1}H−^{1}H dihedral coupling between the β_{IIDMA} bridge protons with the neighboring α_{IIDMA} protons (see Supporting Information Figure S1). Thus the bridge β_{IIDMA} protons appear as a singlet at 4.25 ppm in the ^{1}H NMR spectrum (Figure 1). Therefore, the adjacent α_{IIDMA} protons have no dihedral coupling with the β_{IIDMA} bridge protons and adopt an *endo*-orientation. Logically, the methyleneamine groups should be in an *−exo* orientation. This feature has been frequently illustrated in other isohexide-based polymers.[9,15,17,18,21] Given the fact that the molecular weight of PA5 is in a low range (M_n = 3900 g/mol), the low intensity signals as indicated by dots are assumed to come from the IIDMA end-groups. Overall, we conclude that the stereoconfiguration of IIDMA moieties were preserved during the applied polymerization conditions.

Conformational Analysis of the Copolymers from Solid-State NMR and Quantum-Chemical Calculations. Compared to other step-growth polymers, e.g., polyesters, PAs often have higher melting temperatures mainly due to the strong interchain hydrogen bonds formed between the recurring amide groups. In the solid-state form, the crystal packing of the polymer chain fragments is highly related to the construction of a hydrogen-bonded network. As shown previously, the introduction of DAII or DAIS into the linear polyamides PA 4.10 or PA 4.13 affects the ordered crystal packing and therefore lowers the melting temperatures of the co-PAs.[17−19] The solution ^{1}H NMR spectroscopy, as described above, has been effective in elucidating the molecular structure of the synthesized PAs. In order to study the effect of IIDMA incorporation on the hydrogen-bonding network of the obtained co-PAs, we have employed variable-temperature

dx.doi.org/10.1021/ma302126b | Macromolecules 2012, 45, 9333−9346

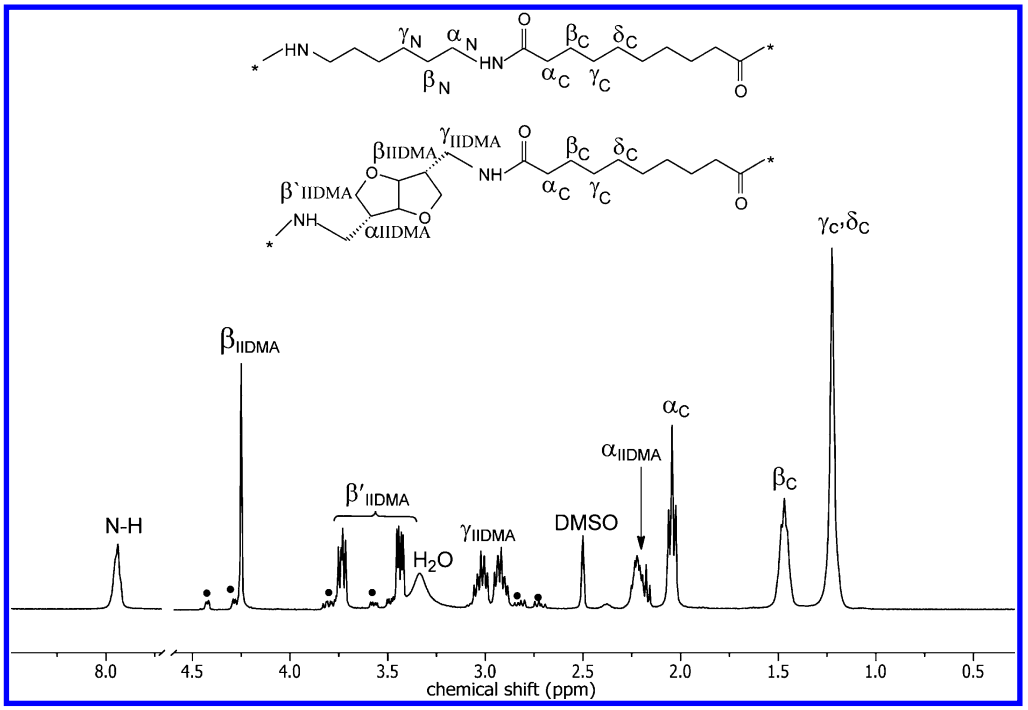

Figure 1. ^{1}H NMR spectrum of the polyamide synthesized from SA and IIDMA (PA5) and the chemical structure of the repeating unit of the homo- and copolyamides. Proton and carbon labels shown in the scheme were used for the analysis of the liquid-state and solid-state NMR spectra. The symbol • indicates the resonances of the IIDMA end-groups.

(VT) ^{13}C{^{1}H} cross-polarization/magic-angle spinning (CP/MAS) NMR spectroscopy. Upon heating from 40 °C to the temperatures close to their corresponding melting points, the hydrogen bonding density of the specimen can be affected, which will be reflected in a change of the NMR resonance signals. Moreover, through careful examination of the resonance signal changes over a wide range of temperatures, additional information concerning the distribution of isohexide-based monomers over crystalline and amorphous phases of the PAs, as well as on the mobility of the polymer chain fragments can be identified. In this work, a particular emphasis is given to the investigation of the existence of different potential IIDMA conformers and their influences on the formation and/or regularity of hydrogen bonding structures by using solid-state NMR spectroscopy techniques. Subsequently quantum-chemical calculations were performed to reveal the most energetically stable IIDMA conformations. Two co-PAs samples, PA3 and PA8 based on SA and BrA, respectively and both having approximately a 50/50 IIDMA/1,6-HDA molar ratio, were characterized for this purpose.

During the heating course of PA3, the resonances from the IIDMA moieties appear as well resolved, albeit broad signals at 86.4, 71.6, and 48.2 ppm for β_{IIDMA}, β'_{IIDMA}, and γ_{IIDMA}, respectively (Figure 2a, Table 2, see Figure 1 for signal assignment). The resonance signals of the methylene proton from the cyclic skeleton (α_{IIDMA}) are difficult to recognize due to overlapping with signals of the alkylene protons from 1,6-HDA units (α_N). All the β'_{IIDMA}, β_{IIDMA}, and γ_{IIDMA} signals show additional minor shoulders that gradually disappear with increasing the temperature, i.e., above ∼150 °C these signals have disappeared. Meanwhile, the remaining major signals from the IIDMA groups become narrower and shift only slightly to lower frequency even when going to the molten state compared to the situation at low temperature. This shows that the IIDMA groups adopt similar conformations over the whole temperature range. At high temperature the reduced ^{13}C line width suggests a decrease in hydrogen bonding density of the polyamides upon heating. Furthermore, the characteristic carbonyl resonances located at ∼173 ppm also appear as a rather broad signal, which gradually decreases in intensity with increasing temperature. In the melt two carbonyl signals with similar intensity appear that can be assigned to the different monomer parts of the copolymer. As reported for PAs synthesized from DAII and DAIS[17−19] the broad and bimodal C═O resonance signals may indicate that the carbonyl groups are involved in two types of hydrogen-bonding environments, most probably referring to the hydrogen bonding occurring in the crystalline and amorphous regions of the sample. However, for PA3 it is not possible to make such an assignment due to similar intensity decay of the both types of signals (Figure 2a) and the occurrence of the carbonyl signals in the melt at the same position.[18,19] Moreover, over the investigated temperature range, the α_N and α_C methylene groups attached to each side of the amide bonds are present as well-defined and narrow signals at 40.5 and 36.7 ppm, respectively, without any visible shoulders (see Figure 2a, Table 2 and Figure 1 for assignment). Interestingly, based on the chemical shift for α_N and α_C below and above the melting temperature, and a comparison to our previous work on PAs synthesized from DAII and DAIS, the number of *trans* conformers in the linear chain fragments of the copolymer PA3 appears to be very limited, i.e., the signals from *trans* conformers should be visible as well resolved resonances at higher frequency.[18,19] Thus, the (VT) ^{13}C{^{1}H} CP/MAS NMR spectra of the PA3 in Figure 2a illustrate that the incorporation of IIDMA significantly increases the transition between *trans* and *gauche* conformers in the methylene moieties of SA and 1,6-HDA, causing the appearance of more *gauche* conformations and a visible reduction in the fraction of *trans* conformers. These observations are in line with FT-IR analysis of PA3 where signals of *gauche* CH_2 scissor vibrations were

dx.doi.org/10.1021/ma302126b | *Macromolecules* 2012, 45, 9333−9346

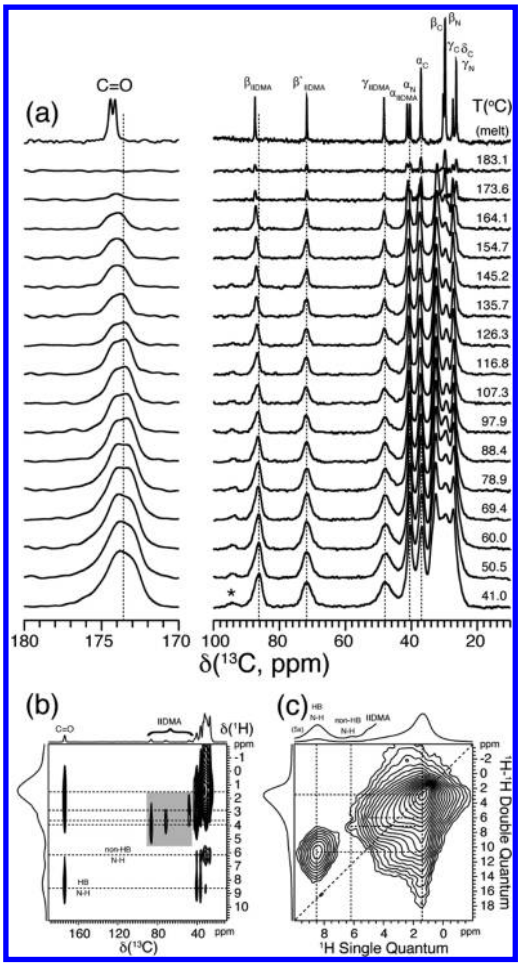

Figure 2. (a) Variable-temperature solid-state $^{13}C\{^1H\}$ CP/MAS NMR spectra recorded at 11.75 T (500 MHz for ^1H) of copolyamide PA3 synthesized from SA, IIDMA, 1,6-HDA with a IIDMA/1,6-HDA molar ratio of 49/51. (b) 2D $^{13}C\{^1H\}$ FSLG-HETCOR spectrum acquired using a 2.0 ms CP step and five FLSG blocks per t_1 increment to improve the ^1H resolution. (c) 2D $^1H-^1H$ DQ-SQ spectrum recorded using a BaBa recoupling period of 67.2 μs. Both 2D spectra were recorded at 20.0 T corresponding to 850.27 MHz for ^1H. The dashed lines in parts b and c illustrate selected cross-peaks and autocorrelation peaks, including hydrogen bonded (HB) and non-hydrogen bonded (non-HB) amide fragments. Assignment of the signals is performed according to Figure 1 and the asterisk in part a indicates the position of a spinning sideband (ssb) from the carbonyl resonance.

emphasized (see below). Further information about the local organization of polymer chains in PA3 can be achieved from the 2D NMR correlation spectra shown in Figure 2, parts b and c. From the 2D $^{13}C\{^1H\}$ FSLG-HETCOR spectrum in Figure 2b the presence of two different hydrogen bond environments can be identified via the correlations of the amide groups to the aliphatic moieties. The non-hydrogen bonded fraction does not show any correlation to the carbonyl groups whereas the hydrogen bonded fraction does. This observation combined with the isotropic chemical shift position of the amide protons at ~8.3 ppm and its correlations to the aliphatic moieties in Figure 2c show that the formed hydrogen bonds in PA3 based on IIDMA are stronger than in PAs synthesized from DAII and DAIS. A possible explanation for the increase in chemical shift, and thereby an increase in hydrogen bond strength,[41] could be that the incorporation of a methylene segment in between the isohexide group and the amide groups enables the hydrogen bonds formation to become organized more perfectly due to improved spatial arrangements, although this occurs at the expense of the occurrence of more *gauche* conformers in the methylene segments as discussed above. The increases in hydrogen bonding strength in turn also explain the higher melting temperatures for the samples studied in this work.

An enhanced mobility of the polymer chain fragments, caused by the increase in *gauche* conformers, is also visible for PA8 synthesized from BrA, 1,6-HDA, and IIDMA. As shown in Figure 3a, the α_N and α_C resonances associated with *gauche* conformers of the linear methylene groups attached to NH and CO motifs at 40.3 ppm and 37.0 ppm are clearly visible throughout the whole temperature range. As also observed for PA3, the intensity of these signals upon heating decreases with only minor displacements visible. Meanwhile, a gradual shift of the relatively broad carbonyl resonance at 173.4 ppm to higher ppm values is observed throughout the temperature range in Figure 3a. This is most likely caused by a reduction in hydrogen bonding efficiency leading to an enhanced mobility of the non-hydrogen bonded amide domains during the course of heating. The $^{13}C\{^1H\}$ CP/MAS NMR spectra of PA8 also includes broad γ_{IIDMA}, β_{IIDMA} and $\grave{\beta}_{IIDMA}$ signals between 47−90 ppm and the α_{IIDMA} resonance located at 40.3 ppm, overlapping with the α_N signal. Again, the narrow ^{13}C line widths of the IIDMA resonances point toward a reduced number of IIDMA conformers over the whole temperature range. From the 2D NMR correlation spectra shown in Figure 3, parts b and c, similar conclusions about the polymer chain organization can be derived for PA8 as for PA3. This includes that the non-hydrogen bonded fraction does not show any correlation to the carbonyl groups and that strong hydrogen bonds are formed, since the amide protons resonate at ~8.6 ppm.

The IIDMA moiety in both PA3 and PA8 show quite narrow ^{13}C resonances suggesting that only a single IIDMA conformer is present. To reveal if this is the case we have performed a 1D potential energy scan (PES). In our previous study on DAII and DAIS fragments, we have shown that the cheaper DFT method B97-D reproduces the potential energy curve obtained

Table 2. ^{13}C Chemical Shifts for the Copolyamides PA3 and PA8 at Different Temperatures

	^{13}C chemical shift (ppm)											
	C=O	α_N	α_C	β_C	γ_C	δ_C	β_N	γ_N	γ_{IIDMA}	β_{IIDMA}	β'_{IIDMA}	α_{IIDMA}
						PA 3						
41.0 °C	173.7	40.5	36.7	22.5−34.5	22.5−34.5	22.5−34.5	22.5−34.5	22.5−34.5	48.2	86.4	71.6	40.5
173.6 °C	174.0	40.2	37.1	22.5−34.5	22.5−34.5	22.5−34.5	22.5−34.5	22.5−34.5	48.4	87.5	71.8	41.3
						PA 8						
41.0 °C	173.4	40.3	37.0	22.3−35.0	22.3−35.0	22.3−35.0	22.3−35.0	22.3−35.0	47.8	86.4	72.2	40.3
164.1 °C	174.0	41.0	37.6	22.3−35.0	22.3−35.0	22.3−35.0	22.3−35.0	22.3−35.0	48.4	87.2	71.6	41.0

dx.doi.org/10.1021/ma302126b | *Macromolecules* 2012, 45, 9333−9346

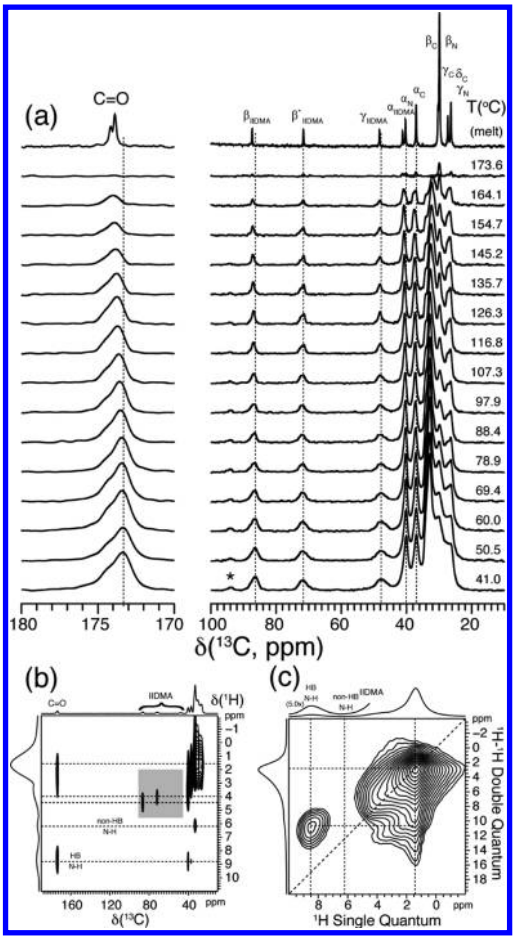

Figure 3. (a) Variable-temperature solid-state $^{13}C\{^1H\}$ CP/MAS NMR spectra recorded at 11.75 T (500 MHz for ^1H) of copolyamide PA8 synthesized from BrA, IIDMA, 1,6-HDA with a IIDMA/1,6-HDA molar ratio 42/58. (b) 2D $^{13}C\{^1H\}$ FSLG-HETCOR and (c) 2D $^1H-^1H$ DQ-SQ spectra recorded as described in the caption of Figure 2. The dashed lines in parts b and c illustrate selected cross-peaks and autocorrelation peaks, including hydrogen bonded (HB) and non-hydrogen bonded (non-HB) amide fragments. Assignment of the signals is performed according to Figure 1 and the asterisk indicates the position of a spinning sideband (ssb) from the carbonyl resonance.

by the more expensive MP2 method.[18,19] For this reason, we have chosen to perform the current study of the conformational profile for the dihedral angle between the amide group and the isohexide fragment in IIDMA at the B97-D level of theory. From the 1D PES it is clear that three conformational minima exist with comparable energies (see Figure S4, Supporting Information). On the basis of this result, a full set of possible conformations have been generated and further optimized at the same level of theory. Contrary to our previous studies of other isohexide derivatives (DAIS and DAII), which showed a large spread of conformers, the incorporation of a methylene segment in between the isohexide and amide groups enables the isohexide fragment to adopt a unique conformation as illustrated in Figure 4a. This conformation is ~10 kJ/mol lower in energy compared to the second most abundant conformer found. In Figure 4a the most abundant conformers of DAII and DAIS fragments are also shown for comparison with the current IIDMA unit. Inspection of these conformers show that the stability of the IIDMA and DAII moieties is due to a pronounced "boat" conformation, which is distorted into the

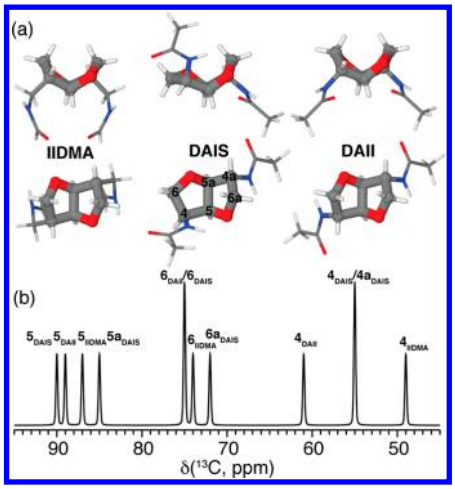

Figure 4. (a) Top and side views of the most stable conformers for the primary diamine (IIDMA) studied in this work, and the diaminoisosorbide (DAIS or *exoendo* oriented diamine) and diaminoisoidide (DAII, *exoexo* oriented diamine) studied in our previous work[17−19] All conformers were found via gas phase MP2/6-311G** level of theory (see Supporting Information for details). (b) Graphical representation of the calculated ^{13}C chemical shifts for all three conformers shown in part a. Note that we have used the nomenclature 4−6 to assign the ^{13}C resonances for nonsymmetric isohexide fragments as shown for DAIS in part a.

"chair" conformation for DAIS.[42] These conformational differences come as a result of the specific stereo configuration of the different isohexide groups. To compare the NMR spectroscopic signatures of all three isohexides we have performed ^{13}C chemical shift calculations at the B97-D/6-311G** level of theory and summarized these as shown in Figure 4b. For the IIDMA unit studied in this work, the calculated ^{13}C chemical shifts are in good agreement with the experimental results in Figures 2 and 3. Clearly, the different isohexide units can be distinguished by their characteristic signals for the anchoring carbons. These carbons are inherently sensitive to a specific conformation of the isohexide moiety ("boat" or "chair"), resulting in a ^{13}C chemical shift spread of 14 ppm in the region from 45 to 65 ppm.

FT-IR Investigation of the Polyamides upon Heating. The hydrogen bonding between the amide moieties of the IIDMA-based polyamides was further investigated by temperature-dependent Fourier transformed infrared (FT-IR) spectroscopy. The applied temperature ranges from 30 °C to slightly above the melting point of the PAs. Three polyamides samples were characterized for this purpose; they are PA3, PA8, and PA6 (PA6.13) with their FT-IR spectra presented in Figures 5−7.

Special attention was given to analyze the intensities of the signals appearing at around 3300 cm^{-1} for all the three PAs, since these signals can be assigned to N−H stretching vibrations. At elevated temperatures, these signals were observed to broaden and their intensities decreased significantly as well. As pointed out by Schroeder[43] and Skrovanek,[44,45] for even- and odd-type nylons, the wavenumber of such bands reflect the average absorptive strength of the hydrogen-bonded N−H groups. The broadening and weakening of these signals upon heating are related to the diminishing of the hydrogen bond density and the formation of non-hydrogen bonded N−H groups. As can be seen from the FT-IR spectra recorded above 180 °C in Figure 5−7, additional signals can be observed at

dx.doi.org/10.1021/ma302126b | *Macromolecules* 2012, 45, 9333−9346

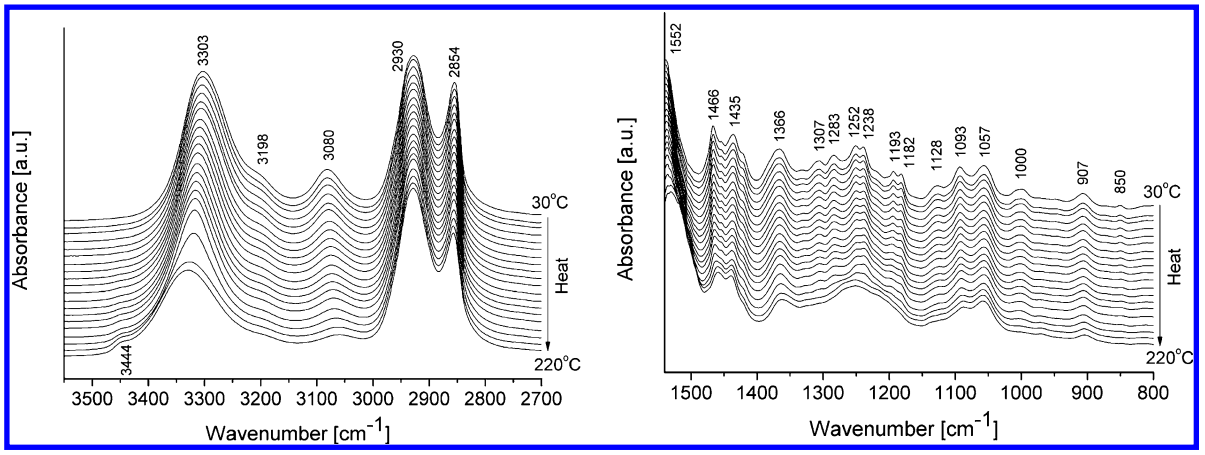

Figure 5. Variable-temperature FT-IR spectra of the copolyamide PA3 recorded from 30−220 °C. PA3 was synthesized from SA, IIDMA, 1,6-HDA with a built-in IIDMA/1,6-HDA molar ratio of 0.49/0.51. The spectra show wave numbers ranging from 3500−2700 cm^{-1} (a) and 1600−800 cm^{-1} (b).

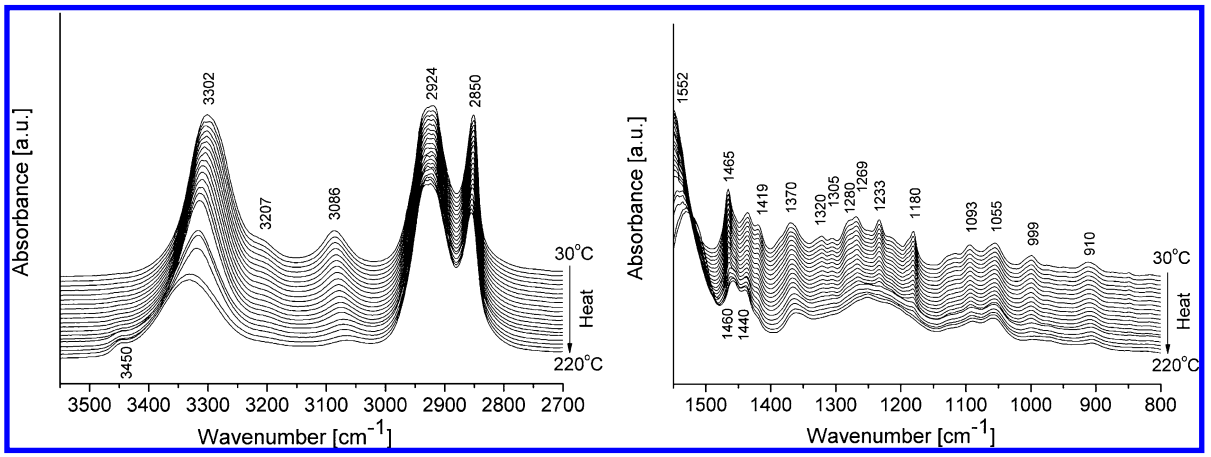

Figure 6. Variable-temperature FT-IR spectra of the copolyamide PA8 recorded from 30−220 °C. PA8 was synthesized from BrA, IIDMA, 1,6-HDA with a built-in IIDMA/1,6-HDA molar ratio of 0.42/0.58. The spectra show wave numbers ranging from 3500−2700 cm^{-1} (a) and 1600−800 cm^{-1} (b).

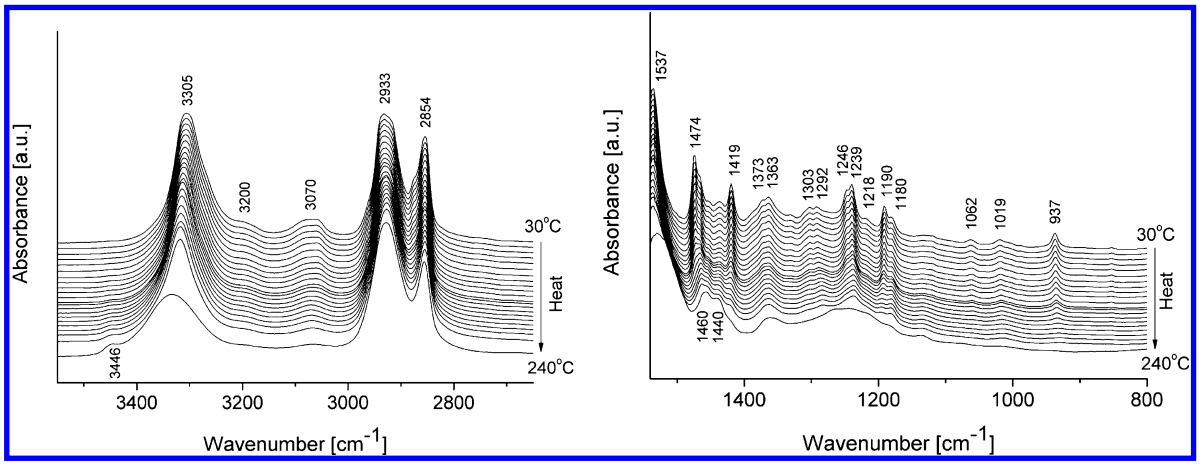

Figure 7. Variable-temperature FT-IR spectra of PA6 (PA 6.13) recorded from 30−240 °C. The spectra show wave numbers ranging from 3500−2700 cm^{-1} (a) and 1600−800 cm^{-1} (b).

around 3444 cm^{-1}. They are the typical indication of the presence of the non-hydrogen bonded N−H groups.

Interesting information about the population of *trans* and *gauche* conformers in the backbone of the polyamides is provided by the signals of C−H vibration from the methylene units attached to each side of the amide groups (-HN-C(O)−). According to literature and our previous findings on the DAII/DAIS-based copolyamides, the C−H vibration from the *trans*-methylene units attached to amine (NH) and carbonyl (C═O) groups show absorptions at wave numbers of 1475 and 1417−

dx.doi.org/10.1021/ma302126b | *Macromolecules* 2012, 45, 9333−9346

1419 cm^{-1}, respectively.[46,47] In the case of PA 6.13, given the pronounced absorptions at 1474 and 1419 cm^{-1}, both the methylene units attached to each side of the amide groups (−HN−C(O)−) are believed to adopt *trans*-conformations (Figure 7b). When IIDMA is incorporated, as shown in Figure 6b for the BrA-based PA8, the presence of the absorption at 1419 cm^{-1} indicates the *trans*-type of methylene units next to C═O; while the methylene units next to N−H in contrast adopt the *gauche*-conformation by showing absorptions at around 1440−1460 cm^{-1} instead of 1474 cm^{-1}. According to Yoshioka et al,[46] due to the lower torsion energy barrier, the conformational changes of the methylene groups next to the CH_2−NH motifs can be easier compared to those attached to the carbonyl group. Similarly, the SA-based PA3 should also adopt gauche conformation, as shown in Figure 5.

Interestingly, as we reported for the DAII-based polyamides, the presence of *exo/exo* oriented isohexide diamines in the backbone of the macromolecules more readily enhances the molecular motion and the induction of gauche type conformers in the linear fragments than their *exo/endo* oriented analogues.[19] IIDMA is a one-carbon extended isohexide diamine, however, due to a similar configuration as DAII the vanishing of the bands corresponding to CH_2 scissoring next to N−H and C═O groups adopting *trans* conformation was already observed for the copolyamides containing around 20 mol % of the bicyclic comonomer (see Supporting Information, Figure S2 and Figure S3).

With regard to the resonances from the isohexide bicyclic skeleton, the FT-IR bands located at 1093 cm^{-1}, 1055−1057 cm^{-1} and 907−910 cm^{-1} are assigned to the asymmetric C−O−C stretching, skeletal C−C stretching and C−CO stretching signals, respectively. It was noticed that these bands exhibit lower intensity when the applied temperatures are close to the melting points, suggesting that IIDMA motifs distribute over both the crystalline and amorphous phases of the materials. Similar phenomena have also been observed for the DAII and DAIS-derived polyamides.[18,19] Further, the signals at 1552 and 1537 cm^{-1} represent the Amide II in-plane N−H deformation with CN and C═O stretch vibration, while the signals corresponding to Amide III and Amide II + III coupled with the hydrocarbon skeleton appear at 1360−1370 and 1180−1190 cm^{-1}, respectively. Since the latter vibrations display a significant decay in their intensity when the recorded temperatures are close to the melting points of the materials, they most probably originate from the temperature-sensitive crystalline phase. Besides, the FT-IR bands corresponding to the methylene motifs of the PAs and related to CH_2 wagging or twisting and skeletal C−C stretch vibrations were found at 1280−1290, 1230−1250, 1218, 1050−1060, and 1019 cm^{-1}, respectively. These modes, excluding signals at 1055−1057 cm^{-1}, display significant changes in their line width at elevated temperature and can be assigned to the crystalline phase of the polyamides.

Thermal Properties of the Polyamides. The thermal stability of the polyamides was investigated by thermogravimetric analysis (TGA). As presented in Table 3, it is evident that the thermal stability of these new biobased materials is dependent on the chemical composition, viz. the molar ratio of IIDMA and 1,6-HDA of the copolyamide, as well as the molecular weight. For the SA- or BrA-based PAs containing less than 50 mol % of IIDMA, the 5% weight loss temperatures of these PAs are in the range of 390−410 °C, which are comparable to those of the reference polyamides PA 6.10 or PA 6.13. However, for the PAs having a IIDMA content greater than 50 mol %, as indicated for the SA-based series, the thermal stability of these materials decreased significantly due to the presence of ether linkages in the isohexide unit. Especially the 5% of weight loss temperature of SA/IIDMA-derived homopolyamide is as low as 323 °C (entry 5, Table 3). A similar trend has been observed by us when proportionally introducing diaminoisoidide (DAII) into PA4,10,[17] as well as upon introducing diaminoisosorbide (DAIS) into PA 4.13.[18] Such an adverse effect on thermal stability of IIDMA incorporation on the copolyamides is assumed to be caused by the generation of crystal structural irregularity of this cyclic moiety into the original linear chains and therefore a reduction of hydrogen bonding density, as shown earlier by the solid-state NMR and FT-IR analyses. Moreover, the relatively low molecular weight of the PA5 (M_n = 3900 g/mol) can also be a factor contributing to the observed sharp decay of thermal stability with increasing IIDMA content.

Table 3. Thermal Stability, Glass Transition Temperatures (T_g), Melt and Crystallization Temperatures (T_m, T_c), and Enthalpy of the Transitions upon Heating (m) and Cooling (c) of the Novel IIDMA-Based Polyamides[a]

entry	$T_{5\%}$ (°C)	T_{max} (°C)	T_g (°C)	T_m (°C)	ΔH_m (J/g)	T_c (°C)	ΔH_c (J/g)
SA/IIDMA/1,6-HDA							
PA1	399.6	456.7	–	222.6	63.1	196.42	55.0
PA2	390.2	460.5	–	210.4	49.5	174.4	52.2
PA3	403.1	449.7	59.5	204.9	36.7	160.4	40.9
PA4	356.7	446.5	66.8	181.6	33.7	123.4	14.1
PA5	323.6	443.8	62.6	157.7	26.1	120.7	22.7
BrA/IIDMA/1,6-HDA							
PA 6	408.7	460.8	–	206.7	71.6	184.3	59.7
PA7	413.1	455.3	–	201.8	53.8	175.3	45.5
PA8	401.8	450.9	–	197.1	54.1	173.9	37.3

[a] $T_{5\%}$ = temperature of 5% mass loss, T_{max} = temperature of maximal rate of decomposition, T_g = glass transition temperature, T_m = melting point, T_c = crystallization temperature, and ΔH = enthalpy of the transition during melting (m) and crystallization (c).

To study the melting (T_m), glass transition (T_g), and crystallization (T_c) temperatures of the synthesized polyamides, differential scanning calorimetry (DSC) analysis was conducted. According to the data presented in Table 3, the presence of IIDMA in the linear PA4.10 and PA4.13 also affect the corresponding melting points of the investigated materials. As the IIDMA content increases from 0 to 100 mol %, the T_m values of the SA-based polyamides progressively decrease from 223 to 158 °C (PA1−5, Table 3, Figure 8). A similar trend was also observed for the BrA-based polyamides (PA6−8, Table 3, Figure 8). An approximate 10 °C reduction of the T_m was observed when 42% of 1,6-HDA was replaced by IIDMA (PA8, Table 3). In the meanwhile, upon increasing the IIDMA content, the melting enthalpies of both series of the copolyamides were reduced accordingly. Compared to PA 6.10 (PA 1, Table 3), the melting enthalpy of the PA IIDMA.10 (PA 5, Table 3) was reduced by more than half. Such trend is in agreement with our previous observation for DAII- and DAIS-derived homo- and copolyamides.[17−19] Such phenomena were explained previously in terms of the formation of less perfect chain packing as well as the reduction of the hydrogen bond density of these isohexide-based copolyamides.[17,48] Additionally, bimodal melting endotherms combined with the presence

dx.doi.org/10.1021/ma302126b | Macromolecules 2012, 45, 9333−9346

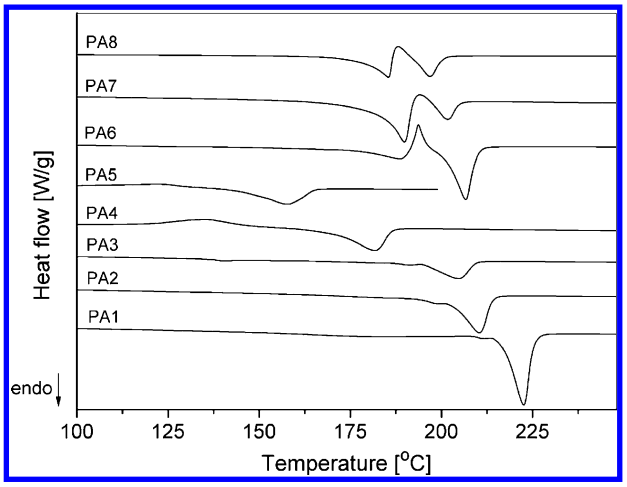

Figure 8. DSC thermograms of the homopolyamides PA 6.10 (PA1), PA IIDMA.10 (PA5), PA 6.13 (PA6), SA, and 1,6-HDA, the IIDMA-based copolyamides PA2, PA3, PA4, BrA, and 1,6-HDA, and the IIDMA-based copolyamides PA7 and PA8. The graph shows the second DSC heating runs with heating rate of 10 °C/min.

of cold crystallization exotherms were observed for the copolyamides synthesized from BrA. This is a typical indication of the existence of imperfect crystals (low melting temperature peak), their melting upon heating and recrystallization into the more perfect crystals (high melting temperature peak). Similar bimodal melting endotherms have also been observed for the DAII-based copolyamides containing more than 40 mol % of DAII, as well for all the copolyamides based on DAIS and BrA-derived copolyamides.[17,18] In contrast, the shapes of the second DSC melting peaks of the SA-based (co)polyamides containing similar percentages of IIDMA appear to be unimodal. This may imply that the crystal structure of SA-based copolyamides is more regularly formed from the melt than the BrA-based copolyamides. Concerning the number of carbon atoms existing in the used comonomers, it is speculated that the combination of brassylic acid and IIDMA/1,6-HDA, viz. the combination of odd (=13) and even (=6) number of carbon atoms, is less favorable for a regular crystal packing than the combination of two monomers with odd numbers of carbon atoms, viz. SA and IIDMA/1,6-HDA.

Closely related to the decrease of T_m and the melting enthalpies, the crystallization temperatures (T_c) and crystallization enthalpies were reduced as well with increasing percentage of IIDMA in the copolyamides. Nevertheless, when the IIDMA content was below 50 mol %, such adverse effect on T_c and crystallization enthalpy is considerably less pronounced than in the cases where the IIDMA content is greater than 50%.

In addition, during the cooling DSC runs at a cooling rate of 10 °C/min (Table 3), pronounced glass transitions were observed for the SA-based copolyamides containing more than 50 mol % IIDMA. From PA3 to PA5, the glass transition temperature of the (co)polyamides increases with the percentage of IIDMA. Compared to the commercialized PA 6.10 (T_g = 50 °C), introduction of IIDMA into PA6.10 raises T_g by 10−17 °C. As extensively shown for other types of isohexide-derived monomers,[1−3] such a T_g-enhancing effect can be understood by the intrinsic rigidity of the bicyclic *cis*-fused tetrahydrofuran rings in IIDMA.

WAXD Analysis of the Polyamides. Wide-angle X-ray scattering measurements were conducted on all the obtained polyamides. As presented in Figure 9, all the synthesized SA-based polyamides are semicrystalline materials, as evidenced by

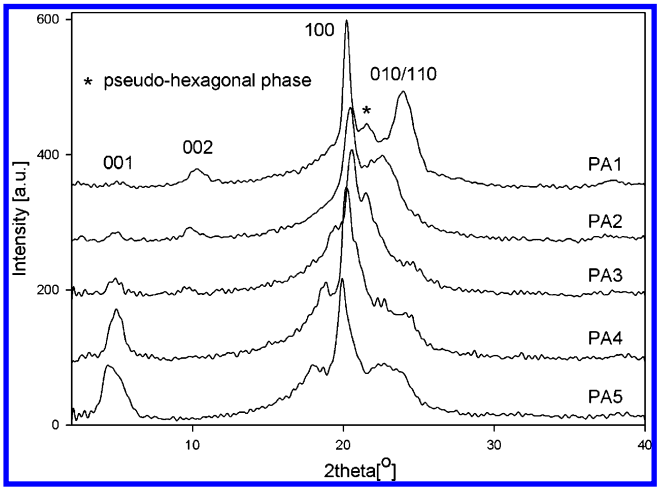

Figure 9. X-ray powder diffraction profiles of 1,6-hexamethylene diamine-, isoidide-2,5-dimethylamine-, and sebacic acid-based polyamides. For compositions of the copolyamides see Table 1.

the sharp scattering signals appearing in their diffractograms recorded at room temperature. The crystallographic structure of these polyamides show strong dependence on the chemical compositions, viz. the molar ratio of IIDMA/1,6-HDA in the copolyamides. When a relatively low content of IIDMA (≤50 mol %, PA2 and PA3) is incorporated, the diffraction profiles of these copolyamides are rather similar to that of the linear PA 6.10 (PA1, Figure 9). Given the presence of four characteristic reflections in the 2θ ranges of 3−7, 10−12, and 18−25° corresponding to the crystallographic planes 001, 002, 100, and 010/110 (Figure 9, Table 4), the crystallographic structures of these polyamides are believed to adopt triclinic forms.[49] The 100 diffraction peak corresponds to the interchain distance, i.e., the distance between two polymer chains lying within the same hydrogen-bonded sheet, while the 010/110 peak corresponds to the intersheet distance, i.e., the distance between two adjacent hydrogen-bonded sheets. The 001 and 002 diffraction peaks give information on the length of the chemical repeat unit. With increasing content of IIDMA in the copolyamides, different trends in the four types of diffraction signals were observed: the 001 and 002 diffraction peaks tend to move toward a region with lower 2θ values, meaning an increase of the *c*-axis dimension of the copolymers due to cocrystallization phenomenon of the comonomers in the same crystallographic lattice; 100 diffraction peaks move toward higher 2θ regions, meaning a decrease of interchain distance within the same hydrogen-bonded sheets; 010/110 diffraction peaks move toward lower 2θ regions, indicating an increase of the intersheet spacing. Additionally, in the diffractogram of PA 6.10 (PA1) shown in Figure 9, we can observe a weak signal with a 2θ value of 21.6°, which is indicative of the presence of a small amount of the pseudohexagonal type of crystals.[49] Comparing to PA1 to PA3, further increasing the IIDMA content to >50 mol % in the SA-based copolymer leads to significant changes of the diffractograms. The diffraction profile of PA4 containing about 68% IIDAM (PA4) displays a comparable diffraction pattern as that of PA IIDMA.10 (PA5). In both cases, there are only two major strong scattering signals appearing in the 2θ regions of 3−7° and 18−25°, respectively. Thus, with

dx.doi.org/10.1021/ma302126b | *Macromolecules* 2012, 45, 9333−9346

Table 4. X-ray Diffraction Spacings of the Copolyamides Based on 1,6-Hexamethylene Diamine, Isoidide-2,5-Dimethylamine, and Sebacic Acid

	2θ (deg)				X-ray diffraction (nm)			
	001	002	100	010/110	001	002	100	010/110
PA1	5.15	10.33	20.22	24.02	1.715	0.856	0.439	0.370
PA2	4.88	9.89	20.42	22.83	1.810	0.894	0.435	0.389
PA3	4.83	9.62	20.55	21.56	1.828	0.919	0.432	0.412
PA4	4.78, 5.13[a]	–	20.30	–	1.848, 1.722	–	0.437	–
PA5	4.32, 5.03[a]	–	19.99	–	2.044, 1.756	–	0.444	–

[a]Due to overlapping of the signals coming from different crystallographic phases, data were derived by deconvolution using WAXSFit software to indicate the possible positions of the diffraction signals.

increasing IDMA content in the compolymides, the crystal structures transform from triclinic (when IIDMA% ≤ 50 mol %, PA1, PA2, and PA3) to a close to hexagonal form (PA4 and PA5). Moreover, as a result of overlapping of the signals coming from different potential crystallographic phases, the scattering signals of PA4 and PA5 in the 2θ range of 3−7° appear to be asymmetric. Hence, two data are given in Table 4 by deconvolution using WAXSFit software to indicate the possible positions of these two peaks for samples PA5 and PA4. In addition, a few low intensity signals were observed to be present at 2θ values of 18°, 22.5°, and 23.6°, respectively, which together with the previous phenomena may indicate the presence of a small percentage of the triclinic crystals as well. In comparison with PA5, the scattering signals of 001 and 100 reflections in the diffraction profile of PA4 were observed to be located at regions of slightly higher 2θ values, suggesting the slightly smaller intersheet and interplane spacings. Nevertheless, given the potential displacements that may exist for the reflection signals of triclinic phase in terms of 2θ values as well as in view of the low amount of this crystallographic form, determining the precise location and displacement of these signals is difficult.

Little knowledge has been available concerning the crystallographic structure of the BrA-based polyamides, e.g. PA 6.13 (PA6). As shown in Figure 10, the diffraction profile of PA 6.13 shows a reflection signal of medium intensity in the 2θ range of 3−7°, as well as two strong reflections in the 2θ range of 18−25°. Such a diffraction pattern resembles those of several linear aliphatic PAs, such as PA 6.10,[49−52] PA4.13,[18] PA 6.12[49,51] or PA 6.18.[49] Therefore, we assume that indexing of individual

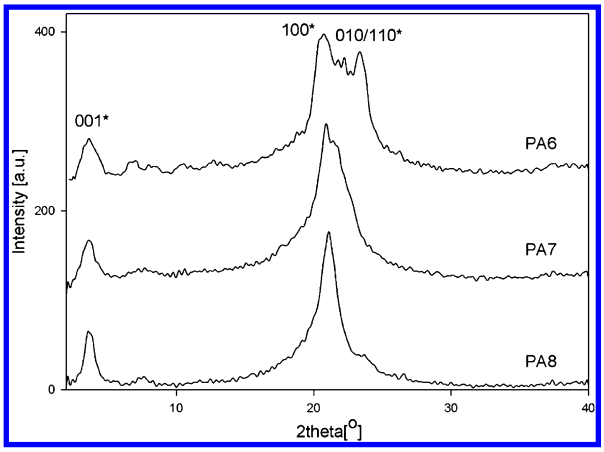

Figure 10. X-ray powder diffraction profiles of the (co)polyamides based on 1,6-hexamethylene diamine, isoidide-2,5-dimethylamine, and brassylic acid.

signals of the BrA-based polyamides should be the same as in the case of SA-based analogous polyamides. In this regard, we assume that the reflection signal located at the 2θ range of 3−7° arises from the 001 plane, while the signals appearing in the 2θ range of 18−25° most probably come from 100 and 010/110 planes of the triclinic crystallographic form.[49] To indicate the uncertainty of the assigned planes for further discussion, individual signals of BrA-based polyamides are marked by asterisks (∗) as shown in Figure 10. In the diffractogram of PA6, several weak signals in the 2θ range of 6−14° were observed for all the three PAs, which might come from the crystallographic planes indexed as 00l. Again, the presence of IIDMA strongly influences the crystallographic structures of the BrA-based polyamides (PA7, PA8). When 18 mol % 1,6-HDA is replaced by IIDMA (PA7, Figure 10), the diffraction signal indexed as 010/110* planes was observed to shift from 24° to a significantly lower 2θ value of 21.8°, suggesting the increase of the intersheet distances (Table 5). Incorporation of 42 mol %

Table 5. X-ray Diffraction Spacings of the (Co)polyamides Based on 1,6-Hexamethylene Diamine, Isoidide-2,5-Dimethylamine, and Brassylic Acid

	2θ (deg)			X-ray diffraction (nm)		
	001*	100*	010/110*	001*	100*	010/110*
PA6	3.67	20.57	23.49	2.406	0.432	0.378
PA7	3.61	20.85	21.83	2.446	0.426	0.407
PA8	3.68	21.11	–	2.399	0.421	–

of IIDMA completely changed the diffractogram as evidenced by the diminishing of the 010/110* signal (in case of the SA-based polyamides, the complete change of the crystallographic structure has taken place only when the IIDMA content is higher than 49 mol %). Therefore, we observe a single reflection in the 2θ range 18−25°, meaning that the IIDMA-rich material crystallized into a close to hexagonal form. Furthermore, with the introduction of IIDMA, the 100* signals show a slight increase in 2θ values, which indicates a decrease of spacing between planes of particular population.

CONCLUSIONS

A combination of melt polymerization and solid state postcondensation (SSPC) has been used as a suitable route to synthesize two novel series of homo- and copolyamides based on the newly developed isoidide-2,5-dimethyleneamine (IIDMA), 1,6-hexamethylenediamine (1,6-HDA), and the renewable sebacic acid (SA) or brassylic acid (BA). The number-average molecular weights (M_n) of the synthesized polyamides are in the range 3900−49000 g/mol. 1D and 2D NMR spectroscopy confirmed the *exo*/*exo* configuration of the

dx.doi.org/10.1021/ma302126b | Macromolecules 2012, 45, 9333−9346

IIDMA moieties in the resulting polyamides. Moreover, the combination of (VT) $^{13}C\{^{1}H\}$ CP/MAS NMR experiments with temperature dependent FT-IR analyses revealed that, as a result of the presence of isohexide building blocks in the backbone of the polyamides, the hydrogen bonding of these semicrystalline materials changed significantly compared to the linear PA6.10 and PA6.13. Due to less regular crystal structures of the IIDMA-containing polyamides, enhanced thermal transitions between *trans* and *gauche* conformations of the alkylene moieties of the SA/BrA and 1,6-HDA were observed. Moreover, it was noticed that the IIDMA moieties are present in both the crystalline and amorphous phases of the copolyamides. Incorporation of the new isohexide-based diamine IIDMA in the linear PA6.10 or PA6.13 on the one hand enhances the glass transition temperature of the polyamides but on the other hand lowers the melting temperatures by forming a less regular hydrogen-bonded network. Computational calculations revealed that, contrary to our previous studies on DAIS- and DAII-based polyamides where bicyclic diamines revealed several different conformers, the presence of methylene units between the isohexide and amide groups in IIDMA favors one stable "boat" conformation of the isohexide fragment. WAXD analysis showed that all the IIDMA-based homo- and copolyamides are semicrystalline materials. The crystallographic structures of the SA-based polyamides are dependent on the molar ratio of the IIDMA and 1,6-HDA moieties. With increasing incoporation of IIDMA, the crystallographic structures of the copolyamides transform from the triclinic form, as in the cases of PA 6.10, PA 6.13 and the co-PAs containing low contents of IIDMA, to a close to hexagonal form for copolyamides containing over 50 mol % of IIDMA-based units. This observation combined with a pronounced increase of the *c*-axis dimension of the copolymers proved the cocrystallization phenomenon of the comonomers in the same crystallographic lattice.

■ ASSOCIATED CONTENT

Ⓢ Supporting Information

NMR and FT-IR spectra and conformational analysis of the polyamides. This material is available free of charge via the Internet at http://pubs.acs.org/.

■ AUTHOR INFORMATION

Corresponding Author

*E-mail: (L.J.W.) l.jasinska@tue.nl; (M.R.H.) mrh@mpip-mainz.mpg.de. Telephone: +31-40-2472527. Fax: +31-40-2463966.

Notes

The authors declare no competing financial interest.

■ ACKNOWLEDGMENTS

The authors acknowledge Prof. H. W. Spiess for helpful discussions. This work forms part of the research program of the Dutch Polymer Institute (DPI, Project Nos. 656 and 685). The financial support from DPI is gratefully acknowledged.

■ REFERENCES

(1) Fenouillot, F.; Rousseau, A.; Colomines, G.; Saint-Loup, R.; Pascault, J. P. *Prog. Polym. Sci.* **2010**, *35*, 578−622.
(2) Kricheldorf, H. R. *Polym. Rev.* **1997**, *37*, 599−631.
(3) Rose, M.; Palkovits, R. *ChemSusChem* **2012**, *5*, 167−176.
(4) Flèche, G.; Huchette, M. *Starch/Stärke* **1986**, *38*, 26−30.
(5) Fletcher, H. G.; Goepp, R. M. *J. Am. Chem. Soc.* **1945**, *67*, 1042−1043.
(6) Fletcher, H. G.; Goepp, R. M. *J. Am. Chem. Soc.* **1946**, *68*, 939−941.
(7) Hockett, R. C.; Fletcher, H. G.; Sheffield, E. L.; Goepp, R. M.; Soltzberg, S. *J. Am. Chem. Soc.* **1946**, *68*, 930−935.
(8) Brandenburg, C. J.; Hayes, R. A. US2003204029 2003.
(9) Storbeck, R.; Rehahn, M.; Ballauff, M. *Makromol. Chem.* **1993**, *194*, 53−64.
(10) Thiem, J.; Luders, H. *Starch/Stärke* **1984**, *36*, 170−176.
(11) Thiem, J.; Lüders, H. *Polym. Bull.* **1984**, *11*, 365−369.
(12) Sablong, R.; Duchateau, R.; Koning, C. E.; De Wit, G.; Van Es, D.; Koelewijn, R.; Van Haveren, J. *Biomacromolecules* **2008**, *9*, 3090−3097.
(13) Noordover, B. A. J.; Haveman, D.; Duchateau, R.; Van Benthem, R. A. T. M.; Koning, C. E. *J. Appl. Polym. Sci.* **2011**, *121*, 1450−1463.
(14) Noordover, B. A. J.; Sablong, R. J.; Duchateau, R.; Van Benthem, R. A. T. M.; Ming, W.; Koning, C.; Van Haveren, J. WO 2008031592, 2008.
(15) Noordover, B. A. J.; Van Staalduinen, V. G.; Duchateau, R.; Koning, C. E.; Van Benthem, R. A. T. M.; Mak, M.; Heise, A.; Frissen, A. E.; Van Haveren, J. *Biomacromolecules* **2006**, *7*, 3406−3416.
(16) Van Haveren, J.; Oostveen, E. A.; Micciché, F.; Noordover, B. A. J.; Koning, C. E.; Van Benthem, R. A. T. M.; Frissen, A. E.; Weijnen, J. G. J. *J. Coat. Technol.* **2007**, *4*, 177−186.
(17) Jasinska, L.; Villani, M.; Wu, J.; Van Es, D.; Klop, E.; Rastogi, S.; Koning, C. E. *Macromolecules* **2011**, *44*, 3458−3466.
(18) Jasinska-Walc, L.; Dudenko, D.; Rozanski, A.; Thiyagarajan, S.; Sowinski, P.; Van Es, D.; Shu, J.; Hansen, M. R.; Koning, C. E. *Macromolecules* **2012**, *45*, 5653−5666.
(19) Jasinska-Walc, L.; Villani, M.; Dudenko, D.; van Asselen, O.; Klop, E.; Rastogi, S.; Hansen, M. R.; Koning, C. E. *Macromolecules* **2012**, *45*, 2796−2808.
(20) Stoss, P.; Hemmer, R. *Adv. Carbohydr. Chem. Biochem.* **1991**, *49*, 93−173.
(21) Wu, J.; Eduard, P.; Thiyagarajan, S.; Jasinska-Walc, L.; Rozanski, A.; Guerra, C. F.; Noordover, B. A. J.; Van Haveren, J.; Van Es, D. S.; Koning, C. E. *Macromolecules* **2012**, *45*, 5069−5080.
(22) Thiem, J.; Lüders, H. *Makromol. Chem.* **1986**, *187*, 2775−2785.
(23) Caouthar, A.; Roger, P.; Tessier, M.; Chatti, S.; Bl−ais, J. C.; Bortolussi, M. *Eur. Polym. J.* **2007**, *43*, 220−230.
(24) Caouthar, A. A.; Loupy, A.; Bortolussi, M.; Blais, J.-c.; Dubreucq, L.; Meddour, A. *J. Polym. Sci., Part A: Polym. Chem.* **2005**, *43*, 2480−2491.
(25) East, A.; Jaffe, M.; Zhang, Y.; Catalani, L. US20080009599 2008.
(26) Gillet, J.-P. WO 2008145921 2008.
(27) Bachmann, F.; Reimer, J.; Ruppenstein, M.; Thiem, J. *Macromol. Rapid Commun.* **1998**, *19*, 21−26.
(28) Thiem, J.; Bachmann, F. *Makromol. Chem.* **1991**, *192*, 2163−2182.
(29) Thiyagarajan, S.; Gootjes, L.; Vogelzang, W.; Van Haveren, J.; Lutz, M.; Van Es, D. S. *ChemSusChem* **2011**, *4*, 1823−1829.
(30) Thiyagarajan, S.; Gootjes, L.; Vogelzang, W.; Wu, J.; Van Haveren, J.; Van Es, D. S. *Tetrahedron* **2011**, *67*, 383−389.
(31) Wu, J.; Eduard, P.; Thiyagarajan, S.; Van Haveren, J.; Van Es, D. S.; Koning, C. E.; Lutz, M.; Fonseca Guerra, C. *ChemSusChem* **2011**, *4*, 599−603.
(32) Bennett, A. E.; Rienstra, C. M.; Auger, C. M.; Lakshmi, K. V.; Griffin, R. G. *J. Chem. Phys.* **1995**, *103*, 6951.
(33) Bielecki, A.; Burum, D. P. *J. Magn. Reson., Ser. A* **1995**, *116*, 215−220.
(34) Van Rossum, B. J.; Förster, H.; De Groot, H. J. M. *J. Magn. Reson.* **1997**, *124*, 516−519.
(35) Feike, M.; Demco, D.; Graf, R.; Gottwald, J.; Hafner, S.; Spiess, H. W. *J. Mag. Reson., Ser. A* **1996**, *122*, 214.
(36) Morcombe, C. R.; Zilm, K. W. *J. Magn. Reson.* **2003**, *162*, 479−486.
(37) Hayashi, S.; Hayamizu, K. B. *Bull. Chem. Soc. Jpn.* **1991**, *64*, 685−687.

(38) Grimme, S. *J. Comput. Chem.* **2006**, *27*, 1787.
(39) Rabiej, M. *Polimery* **2003**, *48*, 288.
(40) Papaspyrides, C. D.; Vouyiouka, S. N., *Solid State Polymerization*. Weily: 2009.
(41) Schmidt, J.; Hoffmann, A.; Spiess, H. W.; Sebastiani, D. *J. Phys. Chem. B* **2006**, *110*, 23204−23210.
(42) Nelson, D. J.; Brammer, C. N. *J. Chem. Educ.* **2011**, *88*, 292−294.
(43) Schroeder, L. R.; Cooper, S. L. *J. Appl. Phys.* **1976**, *47*, 4310−4317.
(44) Skrovanek, D. J.; Painter, P. C.; Coleman, M. M. *Macromolecules* **1986**, *19*, 699−705.
(45) Skrovanek, D. J.; Stephen, E. H.; Painter, P. C.; Coleman, M. M. *Macromolecules* **1985**, *18*, 1676−1683.
(46) Yoshioka, Y.; Tashiro, K. *Polymer* **2003**, *44*, 7007−7019.
(47) Cooper, S. J.; Atkins, E. D. T.; Hill, M. J. *Polymer* **2002**, *43*, 891−898.
(48) Vinken, E.; Terry, A. E.; Hoffmann, S.; Vanhaecht, B.; Koning, C. E.; Rastogi, S. *Macromolecules* **2006**, *39*, 2546−2552.
(49) Jones, N. A.; Atkins, E. D. T.; Hill, M. J.; Cooper, S. J.; Franco, L. *Polymer* **1997**, *38*, 2689−2699.
(50) Bunn, C. W.; Garner, E. V. *Proc. R. Soc. London* **1947**, *44*, 499.
(51) Dreyfuss, P.; Keller, A. J. *Macromol. Sci. Phys.* **1970**, *B4*, 811.
(52) Geil, P. H. *J. Polym. Sci.* **1960**, *44*, 499.